Solvent Effects on Molecular and Ionic Spectra. 6. Hydrogen Bonding and the Delocalized Nature of the First $^1(n,\pi^*)$ Excited State of Pyrazine

J. Zeng,[†] C. Woywod,[‡] N. S. Hush,[†,§] and J. R. Reimers*,[†]

Contribution from the Department of Physical and Theoretical Chemistry, University of Sydney, NSW 2006, Australia, Institute of Physical and Theoretical Chemistry, Technical University of Munich, D-85748 Garching, Germany, and Department of Biochemistry, University of Sydney, NSW 2006, Australia

Received March 13, 1995[⊗]

Abstract: Our method (Parts 1−5[1−6]) for estimating solvent shifts of species which have strong specific interactions (e.g., hydrogen bonding) with the solvent is applied to calculate the absorption and fluorescence solvatochromic (solvent) shifts of dilute pyrazine in water. On the basis of interpretation of solvent shift data, pyrazine in its S_1 $^1(n,\pi^*)$ excited state has been thought to display reduced nuclear symmetry, with the excitation localized on just one of the two nitrogen atoms; this view has also been supported by electronic structure calculations. Such localization could occur, despite the presence of significant through-bond interactions between the nitrogen lone pairs, if the reorganization energy associated with symmetry breaking were sufficiently large. Here, the alternate description is developed for the electronic structure of this excited state of pyrazine based on studies of the free molecule, of pyrazine−water clusters, and of pyrazine in dilute aqueous solution. For the free molecule, extensive *ab initio* Davidson-corrected CASSCF with MRCI calculations strongly suggest a high-symmetry geometry, and verify that this is the correct interpretation of the available experiment data. For pyrazine−water clusters, *only* a high-symmetry model is shown capable of describing the observed high-resolution spectra, and for pyrazine in solution, *only* a high-symmetry model is shown to be capable of interpreting the observed fluorescence solvent shift.

I. Introduction

The nature of pyrazine (1,4-diazabenzene) in its S_1 $^1(n,\pi^*)$ excited state poses a question which has generated much interest over the years. In part, the reason for this lies in the high symmetry of the S_0 ground state, D_{2h}. Most of the vibrational modes are thus not totally symmetric, and many symmetry-lowering possibilities exist: for S_1, distortions which introduce out-of-plane displacements[7−9] and distortions which make the two nitrogen lone-pair atomic orbitals inequivalent[10] have been considered. Additional complexities also arise, since such distortions may change in magnitude under the influence of hydrogen bonding in molecular clusters or condensed phases. While much is known concerning the nuclear symmetry and the underlying electronic structure of S_1, current theories are built on the interpretation of restricted subsets of the available experimental data. Here, we construct a description of this state which is consistent with both high-resolution and low-resolution spectroscopic data covering a variety of molecular environments and describe in detail the nature of the unusual but important pyrazine−water hydrogen bond.

The basic physics of hydrogen-bonding interactions and their effects on molecular spectra were elucidated by Brealey and Kasha[11] in 1955: the ground-state potential S_0 is stabilized by the formation of a hydrogen bond between the "lone pair" (n) orbital of, say, an azine nitrogen atom and a water-hydrogen atom, but in the S_1 excited state the lone pair orbital is depleted of an electron, eliminating the hydrogen bond and hence the additional stabilization. In a hydrogen-bonding environment, additional energy compared to the gas phase is thus required in order to reach the excited state and so a large absorption blue shift is expected, the magnitude of which is related[12] to the ground-state hydrogen bond energy. Alternatively, for a fluorescence spectrum in which light is emitted from the equilibrated S_1 state, no hydrogen bond is present initially and the Franck−Condon transition produces a non-equilibrium final state also without a hydrogen bond and so no hydrogen bond rearrangements are involved and hence a small fluorescence solvent shift is expected. The classic example[6] of this type of interaction occurs between pyridine and water for which the observed[13] absorption and fluorescence solvent shifts are +2500~3000 and −400 cm^{-1} respectively. We[6] have simulated the equilibrium structure of pyridine in both its S_0 and S_1 states in dilute aqueous solution and explicitly verified the appropriateness of the envisaged microscopic structure, as well

[†] Department of Physical and Theoretical Chemistry, University of Sydney.
[‡] Technical University of Munich.
[§] Department of Biochemistry, University of Sydney.
[⊗] Abstract published in *Advance ACS Abstracts*, August 1, 1995.

(1) Zeng, J.; Craw, J. S.; Hush, N. S.; Reimers, J. R. *J. Chem. Phys.* **1993**, *99*, 1482.
(2) Zeng, J.; Hush, N. S.; Reimers, J. R. *J. Chem. Phys.* **1993**, *99*, 1495.
(3) Zeng, J.; Hush, N. S.; Reimers, J. R. *J. Chem. Phys.* **1993**, *99*, 1508.
(4) Zeng, J.; Craw, J. S.; Hush, N. S.; Reimers, J. R. *J. Phys. Chem.* **1994**, *98*, 11075.
(5) Zeng, J.; Hush, N. S.; Reimers, J. R. *J. Phys. Chem.* **1995**, *99*, 10459.
(6) Zeng, J.; Craw, J. S.; Hush, N. S.; Reimers, J. R. *Chem. Phys. Lett.* **1993**, *206*, 323.
(7) Narva, D. L.; McClure, D. S. *Chem. Phys.* **1975**, *11*, 151.
(8) Udagawa, Y.; Ito, M.; Suzuka, I. *Chem. Phys.* **1980**, *46*, 237.
(9) Woywod, C.; Domcke, W.; Sobolewski, A. L.; Werner, H.-J. *J. Chem. Phys.* **1994**, *100*, 1400.
(10) Kleier, D. A.; Martin, R. L.; Wadt, W. R.; Moomaw, W. R. *J. Am. Chem. Soc.* **1982**, *104*, 60.
(11) Brealey, G. J.; Kasha, M. *J. Am. Chem. Soc.* **1955**, *77*, 4462.
(12) Pimentel, G. C. *J. Am. Chem. Soc.* **1957**, *79*, 3323.
(13) Baba, H.; Goodman, L.; Valenti, P. C. *J. Am. Chem. Soc.* **1966**, *88*, 5411.

0002-7863/95/1517-8618$09.00/0

as predicting, without the use of any arbitrarily adjustable parameters, the magnitudes of the resulting shifts.

The diazines have been studied in detail by Baba, Goodman, and Valenti[13] in dilute solution in a variety of hydrogen-bonding and non-hydrogen-bonding solvents. This facilitated the quantification of observed absorption and fluorescence solvent shifts into components arising from the simple dielectric solvation of a chromophore dipole[14-18] and from specific hydrogen bonding. For pyrimidine (1,3-diazabenzene), they concluded that half of the ca. 3000 cm^{-1} observed absorption shift is due to each effect: by simulating the liquid structure[1] and the solvent shift,[3] we explicitly verified this conclusion. Also, Baba *et al.* noted that, similarly to pyridine, large blue absorption solvent shifts and small red fluorescence shifts are produced for the diazines in hydrogen-bonding solvents and concluded that "the hydrogen bond is virtually broken in the (n,π^*) singlet state for the diazines in methanol and water". However, there is an important difference between pyridine and the diazines: while one of two n electrons are removed by excitation in pyridine, only one in four is so removed in a diazine. Hence, if the electrons are equally shared between the two nitrogens, the reduction in the hydrogen bond strength would not be as great, and stable (though weakened) excited state hydrogen bonds could exist. Alternatively, if the interaction energy between the two nitrogen atoms in the diazine is less than the stabilization energy obtained when the molecule distorts to render the two nitrogens inequivalent, point-group symmetry lowering occurs and the (n,π^*) excitation localizes on just one of the two nitrogen atoms; this produces a situation directly analogous to that for pyridine and Baba *et al.*'s conclusion immediately follows. In our terminology, we see that their primary conclusion is thus that in the diazines, symmetry lowering in S_1 occurs, producing localized (n,π^*) excitations.

Historically, in 1965 and before it was generally believed that the lone-pair orbitals in the diazines could only interact via through-space overlap of the atomic orbitals. Clearly, such overlap is very small for pyrimidine and pyrazine, and hence a significant interaction between them was thought unlikely: numerical estimates[19,20] for the coupling between the lone pairs were of the order of 200 cm^{-1}. It was thus inconceivable to think that the inter-nitrogen coupling could be large enough to prevent symmetry lowering from occurring. Based on a large range of data including electronic spectroscopy, photoelectron spectroscopy, and molecular orbital calculations, we now know (see e.g. ref 21) that in situations like this through-bond interactions[22] dominate, and a much larger coupling (of order 4000−10000 cm^{-1}) is expected. Actually, situations in which analogous couplings as small as 200 cm^{-1} are known to occur in very long "molecular wires" such as the α,ω-dipyridyl polyenes[23] $(C_5H_5N)-(CH-CH)_n-(C_5H_5N)$ where $n = 0-4$, or the corresponding Brooker dye ions,[24,25] in which the lone-pair orbitals are separated by 10−20 Å. Given that through-bond couplings in the diazines are now known to be significant, the answer to the question as to whether or not symmetry lowering can occur is not straightforward and requires understanding of the magnitude of the distortive forces which compete with the through-bond coupling to determine the molecular geometry.

For pyrimidine, we have shown[2,3] that symmetry breaking *does not* occur, and hence the excitation remains delocalized in S_1 so that weak but stable hydrogen bonds can form to pyrimidine in its excited state. This work involved the simulation of solvent shifts and comparison of the results with the observed data of Baba *et al.*[13] It is, however, not obvious that the observed data for pyrazine could be similarly interpreted, and all existing theoretical calculations (see e.g. refs 10 and 26) indicate that symmetry breaking in pyrazine does indeed occur.

A key feature for pyrazine is that semiempirical and *ab initio* electronic structure calculations at the Self-Consistent-Field (SCF) level of theory indicate that at D_{2h} nuclear geometries S_1 is unstable[10,27-29] with respect to a reduction of the *electronic* symmetry to C_{2v}: at the ground-state D_{2h} equilibrium geometry, the electronic energy of S_1 evaluated using C_{2v} electronic symmetry is ca.[10] 2 eV *lower* than that evaluated using D_{2h} symmetry. As a consequence of this electronic symmetry reduction, use of a single-determinant description of the electronic wave function results in the (n,π^*) excitation localizing on one of the two nitrogen atoms and the global minimum of the potential surface shifts to a C_{2v} geometry. While such a description is the simplest possible, it is of limited value as the resulting potential surface is not continuously differentiable and so it is not physically realistic. Note that similar results have also be obtained at the Multi-Configurational SCF (MCSCF) level.[26]

The simplest physically realistic[27] electronic wave function for pyrazine S_1 is a two-determinant valence-bond wave function; this explicitly resymmetrizes the localized solutions at the D_{2h} nuclear configuration and provides a much better description of this state than can any single-determinant molecular-orbital wave function. After resymmetrization, the potential surface may have double-minimum character, describing an excited state of reduced symmetry, or may return to a single well, restoring D_{2h} symmetry. Extensive valence-bond calculations have been performed by Kleier *et al.*,[10] their results, shown in Figure 1, do predict a double-minimum potential. This constitutes the key theoretical evidence supporting electron localization in pyrazine S_1.

The simplest model available for describing localization and delocalization is shown in Figure 2. There, the diabatic energies of the two localized (n,π^*) excitations are shown as a function of a (b_{1u}) vibrational coordinate which lowers the point-group symmetry from D_{2h} to C_{2v}. The coupling (resonance energy) is called J while the symmetry-lowering stabilization (reorganization energy) is called λ. Even though significant through-bond interactions are known to occur, the chemically most useful measure of the relative strength of this interaction comes from the ratio $2J/\lambda$: for $2J/\lambda > 1$, the excitations are said to be *strongly* coupled or *delocalized* and the adiabatic potential surfaces have only one minimum, while for $2J/\lambda < 1$, the excitations are said to be *weakly* coupled or *localized* and

(14) Onsager, L. *J. Am. Chem. Soc.* **1936**, *58*, 1486.
(15) Bayliss, N. S. *J. Chem. Phys.* **1950**, *18*, 292.
(16) McRae, E. G. *J. Phys. Chem.* **1957**, *61*, 562.
(17) Liptay, W. *Z. Naturforsch. Teil A* **1965**, *20*, 272.
(18) Rettig, W. *J. Mol. Struct.* **1982**, *84*, 303.
(19) Kerns, D. R.; El-Bayoumi, M. A. *J. Chem. Phys.* **1963**, *26*, 1508.
(20) Moomaw, W. R.; Decamp, M. R.; Podore, P. C. *Chem. Phys. Lett.* **1972**, *14*, 255.
(21) Ohsaku, M.; Murata, H.; Imamura, A.; Hirao, K. *Tetrahedron* **1979**, *35*, 1595.
(22) Hoffmann, R. *Acc. Chem. Res.* **1971**, *4*, 1.
(23) Reimers, J. R.; Hush, N. S. *Inorg. Chem.* **1990**, *29*, 3686.
(24) Reimers, J. R.; Craw, J. S.; Hush, N. S. In *Molecular Electronics—Science and Technology*; Aviram, A., Ed.; AIP: New York, 1992; Vol. II, p 11.
(25) Reimers, J. R.; Craw, J. S.; Bacskay, G. B.; Hush, N. S. *Biosytems.* In press.
(26) Ågren, H.; Knuts, S.; Mikkelsen, K. V.; Jensen, H. J. Aa. *Chem. Phys.* **1992**, *159*, 211.
(27) Wadt, W. R.; Goddard, W. A., III *J. Am. Chem. Soc.* **1975**, *97*, 2034.
(28) Canuto, S.; Goscinski, O.; Zerner, M. *Chem. Phys. Lett.* **1979**, *68*, 232.
(29) Baranov, V. I.; Ten, G. N.; Gribov, L. A. *THEOCHEM* **1986**, *30*, 91.

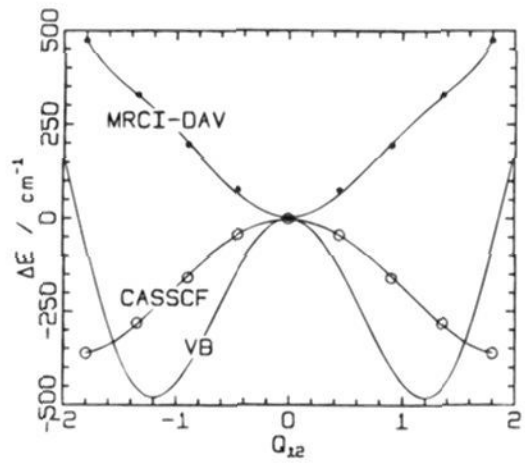

Figure 1. Valence-bond[10] (VB) and CASSCF potential energy surfaces as a function of the displacement (projected onto the ground-state dimensionless normal coordinate Q_{12}) from the respective D_{2h} to C_{2v} minima; the Davidson-corrected MRCI evaluated energy along the CASSCF coordinate is also shown. Energy is expressed as ΔE, the energy relative to that at the D_{2h} configuration. For the CASSCF and MRCI potentials, the points indicate the raw data while the solid lines show the least-square best-fit to a potential containing the terms Q^0_{12}, Q^2_{12}, Q^4_{12}, and Q^6_{12}.

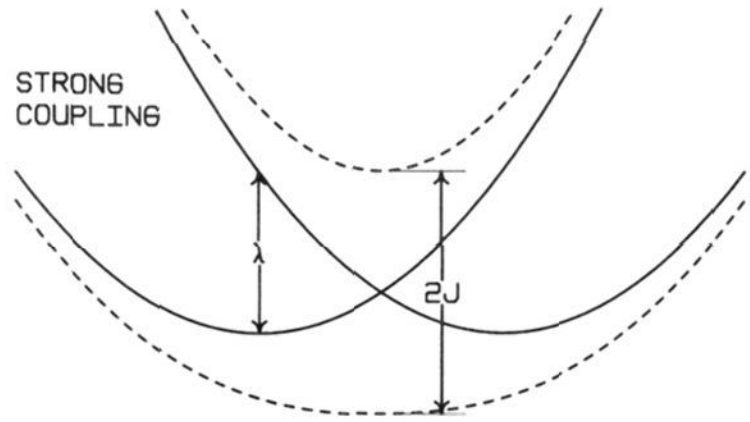

Figure 2. Model energy surfaces for the interaction of localized (n,π^*) excited states: (- - -) Born−Oppenheimer (adiabatic) energies; (—) energies of purely localized (diabatic) states. J is the coupling (resonance interaction energy); λ is the localization stabilization (reorganization) energy. The upper figure depicts strong coupling, $2J/\lambda = 1.5$, while the lower figure depicts weak coupling, $2J/\lambda = 0.5$. The molecular structures corresponding to the localized (C_{2v}) and delocalized (D_{2h}) nuclear structures (see Table 1) are also shown, along with a sketchmatic representation of the n-orbital occupancy: black, 2 electrons (smallest CNC angle), gray, 1.5 electrons; white, 1 electron (largest CNC angle).

the equilibrium geometry has reduced symmetry.[30,31] Note that, for (n,π^*) excitations, both σ and π energies contribute on an equal footing to J and λ, but the distortions involved produce much greater changes in the σ system than in the π system.

Numerically, the value of the coupling J between the localized n orbitals for pyrazine is given (at Koopmans' theorem level) simply as the difference between the two n band centers observed in a photoelectron spectrum; this is[32] $J = 6000$ cm^{-1} (0.8 eV). An alternative measure of J (which is modified slightly by the additional participation of the π system) is the observed splitting between the band centers of the two possible ^{1}(n,π^*) absorptions. Initially,[19,20] these absorptions were believed to be coincident and hence a value of $J \approx 200$ cm^{-1} was thought appropriate; however, both bands have now been clearly identified[10,33−37] establishing beyond doubt that $J = 5500$ cm^{-1}, consistent with the photoelectron value and equal to that observed[38,39] for the splitting of the ^{3}(n,π^*) states. Both simplistic *ab initio* and semiempirical methods (see e.g. refs 40−43) as well as state-of-the-art *ab initio* calculations[44−47] confirm these assignments and do predict a coupling of around this value. Clearly, we see that the lone-pair interaction is not trivially small and hence λ must also be large in order to affect localization.

The key question as to whether or not a symmetry-breaking nuclear distortion occurs in S_1 is answerable from the results of high-resolution absorption and emission spectroscopy. Franck−Condon progressions can only occur in modes which are symmetric with respect to all symmetry operators common to both S_0 and S_1. No progressions in any mode which localizes the (n,π^*) excitation are readily identifiable.[7,8,33,35] As discussed by Kleier *et al.*,[10] this is substantial evidence indicating that the localized ^{1}(n,π^*) excitations are in fact strongly coupled in pyrazine (i.e., in our terminology, $2J > \lambda$); they suggested, however, that the experimental data could also be consistent with a scenario in which a double-well potential existed, with the well being so shallow as to barely sustain zero-point vibration. We consider this suggestion quantitatively in Section 2d. Their valence-bond calculations, which lead to the conclusion that S_1 has a double-minimum potential, do depict J accurately and thus if S_1 is indeed highly symmetric then these calculations must considerably overestimate λ, the energy gain on localization. In this case, the (latent) tendency to localize would have its own effects on the observed spectra, and could easily account for the observed depression in the key b_{1u} vibrational mode, ν_{12}, from[48] 1021 cm^{-1} in S_0 to what is believed[10,34,49] to be 636 cm^{-1} in S_1. In Figure 2, the physical origin of such a depression is clearly manifest. Indeed, the effect of the finite λ is to introduce vibronic coupling between the

(30) Hush, N. S. *Chem. Phys.* **1975**, *10*, 361.
(31) Reimers, J. R.; Hush, N. S. *Chem. Phys. Lett.* In preparation.
(32) Fridh, C.; Åsbrink, L.; Jonsson, B. ö.; Lindholm, E. *Int. J. Mass Spectrom. Ion Phys.* **1972**, *8*, 101.
(33) Zalewski, E. F.; McClure, D. S.; Narva, D. L. *J. Chem. Phys.* **1974**, *61*, 2964.
(34) Esherick, P.; Zinsli, P.; El-Sayed, M. A. *Chem. Phys.* **1975**, *10*, 415.
(35) Bolovinos, A.; Tsekeris, P.; Philis, J.; Phantos, E.; Andritsopoulos, G. *J. Mol. Spectrosc.* **1984**, *103*, 240.
(36) Innes, K. K.; Ross, I. G.; Moomaw, W. R. *J. Mol. Spectrosc.* **1988**, *132*, 492.
(37) Okuzawa, Y.; Fujii, M.; Ito, M. *Chem. Phys. Lett.* **1990**, *171*, 341.
(38) Inoue, A.; Webster, D.; Lim, E. C. *J. Chem. Phys.* **1980**, *72*, 1419.
(39) Fischer, G. *Can. J. Chem.* **1993**, *71*, 1537.
(40) Clementi, E. *Chem. Rev.* **1968**, *68*, 341.
(41) Del Bene, J.; Jaffé, H. H. *J. Chem. Phys.* **1968**, *48*, 1807, 4050.
(42) Del Bene, J.; Jaffé, H. H. *J. Chem. Phys.* **1969**, *50*, 563.
(43) Del Bene, J. E. *J. Am. Chem. Soc.* **1975**, *112*, 9405.
(44) Walker, I. C.; Palmer, M. H. *Chem. Phys.* **1991**, *153*, 169.
(45) Fülscher, M. P.; Andersson, K.; Roos, B. O. *J. Phys. Chem.* **1992**, *96*, 9204.
(46) Seidner, L.; Stock, G.; Sobolewski, A. L.; Domcke, W. *J. Chem. Phys.* **1992**, *96*, 5298.
(47) Zhu, L.; Johnson, P. *J. Chem. Phys.* **1993**, *99*, 2322.
(48) Innes, K. K.; Byrne, J. P.; Ross, I. G. *J. Mol. Spectrosc.* **1967**, *22*, 125.
(49) Knoth, I.; Neusser, H. J.; Schlag, E. W. *Z. Naturforsch. A* **1978**, *34*, 979.

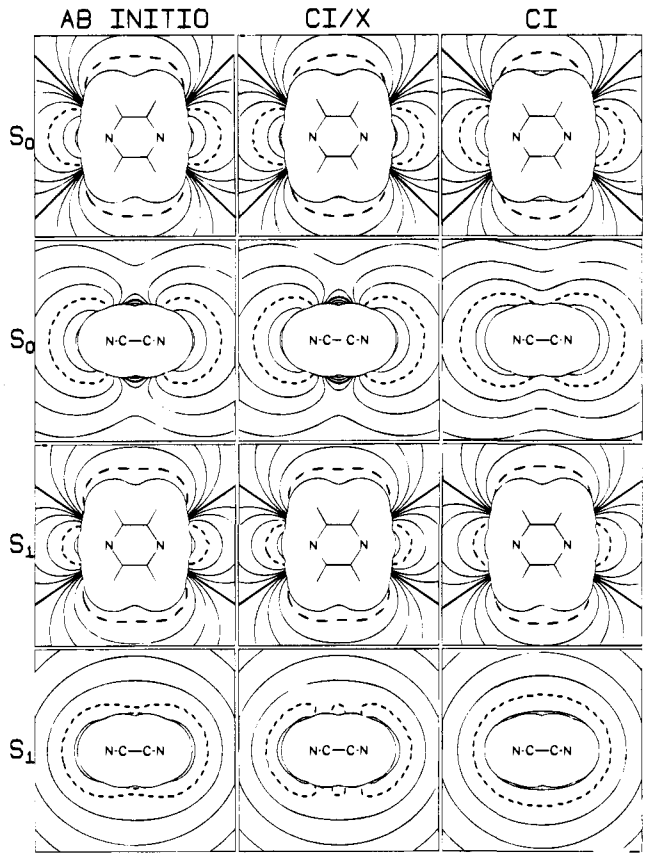

Figure 3. Contours in the molecular plane and normal to it of the *ab initio* CI ESP for S_0 and S_1, as well as the corresponding contours evaluated from the fitted charge distributions used in the potentials Φ_{CI}, $\Phi_{CI/X}$, Φ'_{CI}, and $\Phi'_{CI/X}$. Results are shown only outside the shell at 1.4 times the atom van der Walls radii; contour values are (bold) 0; (- - -) −8; (—) ±32, ±16, ±4, ±2, ±1 kcal mol^{-1} e^{-1}.

two adiabatic $^1(n,\pi^*)$ states, and its magnitude can be obtained using[31,50]

$$\frac{\nu(S_1)}{\nu(S_0)} = \left(1 - \frac{\lambda}{2J}\right)^{1/2} \quad (1)$$

This gives $\lambda/2J = 0.60$ so that if $J = 5500$ cm^{-1} then $\lambda = 6600$ cm^{-1}, in itself quite large in magnitude yet not quite large enough.

When pyrazine forms hydrogen bonds to water, the bond strength increases as the number of electrons in the lone-pair atomic orbital involved in the hydrogen bonding increases, i.e., as the degree of localization increases.[13,51] In this way, hydrogen bonding increases the total reorganization energy by making the localized configurations more stable, and it is possible that $2J/\lambda < 1$ in pyrazine−water clusters or in solution, giving rise to a qualitatively different electronic structure for pyrazine S_1. In the extreme limiting case of no hydrogen bonding at all in the delocalized case, λ would increase by the hydrogen bond strength of (at most) 2000 cm^{-1} to 8600 cm^{-1} but would still be less than $2J$, 11000 cm^{-1}. Hence, based on this analysis, hydrogen-bonded pyrazine is not expected to exhibit localized (n,π^*) excitations; a similar scenario is also found for pyrimidine.[2]

Experimentally, stable pyrazine mono- and dihydrates have been observed for pyrazine in its lowest $^3(n,\pi^*)$ state in low-temperature doubly-dilute glasses[51] and solid neon,[52] and spectral shift data indicate that the dihydrates contain one water molecule hydrogen bonded to each nitrogen atom. Phosphorescence excitation spectra of these complexes show well-resolved $S_0 \rightarrow S_1$ absorption lines, and these are especially well resolved in the spectra of Rossetti and Brus[52] in solid neon at 4.2 K. S_1 is seen to form stable hydrogen bonds with either one or two water molecules, and no new progressions in intermolecular modes (a key signature of broken or significantly weakened excited state hydrogen bonds[12]) are seen. While these results confirm the essentially delocalized nature of both the singlet and triplet (n,π^*) states, evidence of localization-promoting forces remains, producing a much larger blue shift of the absorption origin from the addition of the second water hydrate (650 cm^{-1}) than from the addition of the first (340 cm^{-1}). Note also that pyrazine−water clusters have been observed in a molecular beam by Wanna, Menapace, and Bernstein[53] using fluorescence excitation spectroscopy, but little information is available. These authors failed to observe the corresponding two-color time-of-flight mass spectroscopy signal: although this may by due to the clusters being unstable in the excited state, given the neon matrix isolation results,[52] this is more likely due to known experimental difficulties.[53,54]

In this paper, we examine the hypothesis[13] that the observed solvent (solvatochromic) shifts in solution can only be interpreted in terms of localized excitations. A theory is developed which is capable of describing the properties of isolated pyrazine, pyrazine−water clusters, and dilute pyrazine solutions. This leads to a consistent description of the electronic structure of pyrazine and elucidates fundamental properties of hydrogen bonding in excited states. Five steps are involved, and although parameters are used or options considered in every step of the modeling, at no stage is any *arbitrarily* adjustable parameter introduced whose value is set in order to fit experimental data; in particular, no spectroscopic data is used at all. These steps are the following: (1) the evaluation *ab initio* of the electronic structure of pyrazine in its S_0 and S_1 states in the gas phase, (2) the generation of pyrazine−water effective pair potentials for both states, (3) the evaluation of the structure and spectroscopic properties of pyrazine−water clusters, (4) the evaluation of the structure of aqueous S_0 and S_1 pyrazine, and (5) the evaluation of the absorption and fluorescence solvent shifts. Previously, this technique has been successfully applied to study solvent shifts and chemical processes in pyridine,[6] pyrimidine,[1-3] $Fe^{2+}(H_2O)_6$[4], $Ru^{2+}(NH_3)_5$−pyridine,[5] and $Ru^{2+}(NH_3)_5$−pyrazine.[55]

Step 1, the accurate determination of the electronic structure of pyrazine in both electronic states, is in principle feasible using modern *ab initio* techniques which first perform a Complete-Active-Space SCF (CASSCF) calculation, which could possibly involve use of a Self-Consistent Reaction Field[26] (SCRF), followed by either a large Multi-Reference singles and doubles Configuration-Interaction (MRCI) calculation[9,44] or a perturbation-theory calculation[45] (CASPT2). At the MRCI level, it is known[44] that no additional lowering of energy is required (as is the case at the SCF level[10]) in going from D_{2h} to C_{2v} electronic symmetry in order to reproduce the observed $S_0 \rightarrow S_1$ transition energy. Also, it has been suggested from spectroscopic data[7,8] that pyrazine in S_1 does indeed distort slightly along non-totally-symmetric coordinates. The envisaged displacement is, however, out-of-plane in nature and is postulated to lower the

(50) Hush, N. S. *NATO Adv. Study Inst. Ser., Ser. C* **1980**, *58*, 151.
(51) Marzzacco, C. *J. Am. Chem. Soc.* **1973**, *95*, 1774.
(52) Rossetti, R.; Brus, L. E. *J. Chem. Phys.* **1979**, *70*, 4730.
(53) Wanna, J.; Menapace, J. A.; Bernstein, E. R. *J. Chem. Phys.* **1986**, *85*, 1795.
(54) Warina, J.; Bernstein, E. R. *J. Chem. Phys.* **1986**, *84*, 927.
(55) Zeng, J.; Hush, N. S.; Reimers, J. R. *J. Phys. Chem.* In preparation.

symmetry from D_{2h} to C_{2h} while maintaining the equivalence of the two nitrogen lone-pair orbitals. Physically, the origin of such a displacement could be the observed strong vibronic coupling between the S_1 and S_2 electronic states: an indication of the high quality now attainable using *ab initio* MRCI calculations is the recent description by Woywod *et al.*[9] of this process, including a mapping of the important conical intersection between S_1 and S_2 and a complete *a priori* simulation of the complicated vibronic spectra of S_1.

The methods used in all five steps are described in Section 2; this includes details of the pyrazine gas-phase electronic structure calculations. Solvent-shift and solvent-structure calculations are described for pyrazine-water clusters and for pyrazine in dilute solution in Sections 3 and 4, respectively.

2. Calculation Methods

(a) Solvent-Shift Evaluation. The method used to evaluate the solvent shift at the centre of the pyrazine $^1(n,\pi^*)$ absorption and fluorescence bands is described in detail elsewhere.[3] Briefly, the method involves two stages and uses different energy expressions for each. In the first stage, standard Monte Carlo simulations are performed to determine the structure of liquid water around pyrazine in both its ground and excited electronic states. This involves the use of effective pair potentials to describe the water−water and water−pyrazine interactions in the condensed phase. In the second stage, sample configurations are selected from the Monte Carlo simulations and analyzed to determine the vertical (Franck−Condon) solvent shift. Here, it is in general necessary to evoke the best-possible description of the electrostatic component of the intermolecular potential, and we use a fully polarizable n-body function. Also, spherical boundary conditions are used during this stage, enabling very-long-range electrostatic interactions to be modeled using Friedman's reaction field technology,[56] suitably modified[3] for vertical excitation. This approach treats the intermolecular interactions as perturbations to the electronic structure of the chromophore; here, we ignore hyperpolarizabilities and intermolecular charge-transfer processes as they are believed to be unimportant for pyrazine in water, and in general we ignore dispersive interactions as they are very expensive to evaluate and contribute only of the order of a few hundred wavenumbers to the solvent shift. The molecular parameters used[57,58] for water during the solvent-shift evaluation are the following: gas-phase atomic charges $q_H = 0.33$ e, $q_O = -0.66$ e, dielectric constant $\epsilon = 78.5$, refractive index $n = 1.333$, and isotropic polarizability $\alpha = 9.6164$ au. Other methods for evaluating solvent shifts are available, including (1) self-consistent reaction field theory (see e.g. ref 26), which is fast and efficient for nonpolar solvents but cannot treat specific interactions such as hydrogen bonding,[3,5,6] (2) simply employing the effective pair potentials used to generate the liquid structure to evaluate the solvent shift either classically[59,60] or semiclassically,[61] which has the disadvantage that such potentials approximate the electrostatic interactions too crudely, and (3) full quantum liquid simulations,[62] which are very general and include all interactions but are very expensive and are generally based on semiempirical electronic structure calculations which describe intermolecular interactions usually poorly.[63]

(b) Liquid Simulations. Full details of the simulation techniques used, including error analysis methods, are given elsewhere. Briefly, convergence accelerated[64] rigid-molecule constant number, temperature, and pressure (NPT ensemble[65]) Monte Carlo[66,67] calculations[1,2] are performed at $T = 298$ K and $P = 1$ atm for a sample containing one pyrazine molecule and 102 water molecules. Periodic truncated octahedral boundary conditions[68−70] are used; these provide many advantages.[1] Equilibration is performed for at least 10^7 moves, considerably longer than the longest relaxation "times" found in such systems,[1] and a total of either 4×10^7 or 20×10^7 configurations are generated. Error bars quoted are $1 - \sigma$ and are based on analysis subsamples of size $2-10 \times 10^6$. Every 200th configuration is analyzed in order to determine the radial distribution functions, and every 2000th configuration is subsequently analyzed to determine the solvent shift. Pairwise additive intermolecular potentials are constructed using Kollman's (second) function form,[71] which specifies the TIP3P[72] water−water potential and includes contributions from both Lennard-Jones and Coulomb interactions. For the Lennard-Jones contributions, we use the same parameter set as described previously.[1] Note that, even though Kollman's function is intended for use only for molecules in their ground state, we use the same Lennard-Jones terms for both the ground and excited states. For the solvent shift of pyridine and pyrimidine in water,[1−3,6] we have shown that the results obtained are quite sensitive to the intermolecular potentials used, and that the above assumptions are consistently reliable.

The Coulombic part of Kollman's intermolecular potential is specified to be the interaction between the TIP3P water charges and (electronic-state dependent) atomic pyrazine charges. These are usually determined by fitting[1] the SCF *ab initio* electrostatic potential (ESP) obtained using the double-ζ plus polarization[73] (DZP) basis set. Indeed, we generate atomic charges in this fashion, but because of its high symmetry, pyrazine forms an interesting special case with atomic-charge-only models having insufficient flexibility to adequately describe the ESP. We consider a range of possible electrostatic potentials for both the ground and excited states, as described later. In particular, potentials corresponding to both localized and delocalized excited states are generated.

(c) Pyrazine−Water Cluster Properties. Although the pyrazine−water effective pair potentials generated are intended for use only in condensed phases and are not strictly applicable to multiple phases,[74,75] we use them to study properties of pyrazine·(H_2O) and pyrazine·$(H_2O)_2$. This will, at least, facilitate understanding of the results of the liquid simulations; also, we have found[2,6] that calculations of this type can at least qualitatively interpret the often perplexing results of cluster experiments. Cluster calculations using effective pair potentials always[1,6,74] overestimate the binding energies, underestimate the hydrogen bond lengths, and (incorrectly, given the results of ref 51) assume that the two water molecules add essentially independently to symmetric bifunctional acceptors like delocalized pyrazine.

(d) Gas-Phase Electronic Structure. Two sets of *ab initio* electronic structure calculations are performed in order to determine the properties of the ground (S_0) and first excited (S_1, $^1(n,\pi^*)$) states of pyrazine. In the first set, SCF calculations are performed for S_0 at its SCF-calculated[10] D_{2h} equilibrium geometry in the manner recommended[71,76,77] for use in constructing intermolecular potentials. Similarly, assuming the $^1(n,\pi^*)$ excitation to be local in nature, SCF calculations are also performed for S_1 at the equilibrium geometry

(56) Friedman, H. L. *Mol. Phys.* **1975**, *29*, 1533.
(57) Eisenberg, D.; Kauzmann, W. *The Structure and Properties of Water*; Oxford: Oxford, 1969.
(58) Weast, R. C., Ed. *Handbook of Chemistry and Physics*, 55th ed.; Chemical Rubber Company: Cleveland, 1974.
(59) Bergsma, J. P.; Berens, P. H.; Wilson, K. R.; Fredkin, D. R.; Heller, E. J. *J. Phys. Chem.* **1984**, *88*, 612.
(60) DeBolt, S. E.; Kollman, P. A. *J. Am. Chem. Soc.* **1990**, *112*, 7515.
(61) Reimers, J. R.; Wilson, K. R.; Heller, E. J. *J. Chem. Phys.* **1983**, *79*, 4749.
(62) Luzhkov, V.; Warshel, A. *J. Am. Chem. Soc.* **1991**, *113*, 4491.
(63) Karelson, M. M.; Zerner, M. C. *J. Am. Chem. Soc.* **1990**, *112*, 9405.
(64) Kincaid, R. H.; Scheraga, H. A. *J. Comput. Chem.* **1982**, *3*, 525.
(65) McDonald, I. R. *Mol. Phys.* **1972**, *23*, 41.
(66) Metropolis, N. A.; Rosenbluth, A. W.; Rosenbluth, M. N.; Teller, A. H.; Teller, E. *J. Chem. Phys.* **1953**, *21*, 1087.
(67) Wood, W. W.; Parker, F. R. *J. Chem. Phys.* **1957**, *27*, 720.
(68) Adams, D. J. *Chem. Phys. Lett.* **1979**, *62*, 329.
(69) Adelman, S. A. *J. Chem. Phys.* **1980**, *73*, 3145.
(70) Allen, M. P.; Tildesley, D. J. *Computer Simulation of Liquids*; Clarendon: Oxford, 1987.
(71) Cieplak, P.; Kollman, P. A. *J. Am. Chem. Soc.* **1988**, *110*, 3734.
(72) Jorgensen, W. L.; Chandrasekhar, J.; Madura, J. D.; Impey, R. W.; Klein, M. L. *J. Chem. Phys.* **1983**, *79*, 926.
(73) Dunning, T. H., Jr.; Hay, P. J. In *Modern Theoretical Chemistry*; Schaefer, H. F., III, Ed.; Plenum: New York, 1976, Vol. 3.
(74) Reimers, J. R.; Watts, R. O.; Klein, M. L. *Chem. Phys.* **1982**, *64*, 95.
(75) Reimers, J. R.; Watts, R. O. *Chem. Phys.* **1984**, *91*, 201.
(76) Weiner, S. J.; Kollman, P. A.; Case, D. A.; Singh, U. C.; Ghio, C.; Alagona, G.; Profeta, S., Jr.; Weiner, P. *J. Am. Chem. Soc.* **1984**, *106*, 765.
(77) Weiner, S. J.; Kollman, P. A.; Nguyen, D. T.; Case, D. A. *J. Comput. Chem.* **1986**, *7*, 230.

Table 1. Cartesian Coordinates, in Å in Terms of the Molecular Long (L), Short (S), and Normal (N) Axes, for the N, C, and H Atoms of Pyrazine as well as for an Additional Point Charge X That Are Used in Various S_0 Potentials Φ and S1 Potentials Φ', See Text

potentials	atom	L	S	N
Φ_{SCF}, $\Phi_{SCF/X}$,	N	±1.4553	0	0
Φ_{CI}, $\Phi_{CI/X}$,	C	±0.6887	±1.1457	0
Φ'_{CI}, $\Phi'_{CI/X}$	H	±1.2283	±2.0928	0
Φ'_{SCF}, $\Phi'_{SCF/X}$	N	1.3728	0	0
	N	−1.5511	0	0
	C	0.6855	±1.2382	0
	C	−0.6855	±1.2139	0
	H	1.2253	±2.1852	0
	H	−1.2253	±2.1608	0
$\Phi_{SCF/X}$	X	±0.7881	±0.5259	±0.8856
$\Phi_{CI/X}$	X	±0.7270	±1.1844	±0.1658
$\Phi'_{SCF/X}$	X	1.2624	±0.5622	±0.1127
	X	0.2067	±0.6154	±0.4583
$\Phi'_{CI/X}$	X	±0.9567	±0.3276	±1.0361

optimized by Kleier *et al.*[10] using valence bond theory. A double-ζ plus polarization basis set[73] containing 110 basis functions is used via HONDO[78] in both cases, and the equilibrium geometries are shown in Table 1.

In the second set, calculations are performed at the highest currently feasible level, a level which has been shown[9] to be capable of reproducing the relative energies of these states as well as of interpreting the complex conical intersection of the S_1 and S_2 $^1(\pi,\pi^*)$ states. These calculations have been described in detail elsewhere,[9] but briefly the same basis set is used as above and MRCI calculations based on a CASSCF wave function are performed using MOLPRO.[79] For the (a_g, b_{3u}, b_{2u}, b_{1g}, b_{1u}, b_{2g}, b_{3g}, a_u) orbitals in D_{2h} symmetry, (5, 0, 4, 0, 4, 0, 3, 0) specifies the CASSCF inactive orbitals while (1, 2, 0, 1, 1, 2, 0, 1) species the active orbitals into which 10 electrons are distributed, and (4, 0, 2, 0, 3, 0, 2, 0) orbitals are frozen in the MRCI. Again, two geometries are used in these calculations, one symmetric and one asymmetric. As for the SCF calculations, the asymmetric geometry used is Kleier *et al.*'s[10] valence-bond optimized S_1 geometry, but the symmetric geometry used is actually the DZP-MP2 structure rather than the DZP-SCF structure shown in Table 1, but the differences are not large.

At the Davidson-corrected MRCI level of theory, S_1 is calculated[9] to lie 4.22 eV vertically above S_0 at its DZP-MP2 geometry, close to the experimental value of 3.94 eV. At this geometry, we have explicitly verified that these calculations are independent of the electronic point-group symmetry used: no instabilities occur, and the potential surface is continuously differentiable if the active space defined above is employed and CASSCF averaging over S_0, S_1, and S_2 is performed.

Attempts have also been made to optimize the structure of S_1. With the nuclear symmetry constrained to D_{2h} a minimum is found at the UHF-MP2/DZP level of approximation which lies 0.099 eV below the vertical excitation energy (the geometry is quite similar to that obtained by Zhu and Johnson[47]). This energy lowering corresponds well to the observed absorption band-center to band-origin difference of 0.11 eV and indicates that symmetry lowering cannot significantly stabilize the S_1 state. Similarly, optimization in D_{2h} symmetry using the CASSCF method followed by a Davidson-corrected MRCI energy calculation gave an energy lowering of 0.109 eV, again in excellent agreement with experiment. When all symmetry constraints are relaxed, however, the CASSCF method yields a minimum for S_1 of C_{2v} symmetry with the (n,π^*) excitation localized on one of the two nitrogen atoms. This equilibrium geometry corresponds essentially to a displacement of 1.8 dimensionless units along normal coordinate ν_{12} from the minimum of the electronic ground state. Averaging over the states $^1A_1$, $^1B_1$, and $^1B_2$ results in a CASSCF stabilization energy of 0.045 eV (360 cm^{-1}) compared to the D_{2h}-optimized CASSCF energy. This result is similar to that obtained by Kleier *et al.*[10] using valence bond theory, and both potential surfaces are shown in Figure 1. Note that, in this figure, the abscissa is actually the projection of the displacement between the respective high- and low-symmetry structures projected onto the dominant ground-state dimensionless normal coordinate Q_{12}. However, the Davidson-corrected MRCI energy of S_1 calculated along the path from the CASSCF-optimized D_{2h} to C_{2v} structures increases monotonically to 0.059 eV (470 cm^{-1}); this energy is also shown in Figure 1. Hence, these calculations indicate that the stabilizing effect of a localizing distortion for S_1 observed at the valence-bond and CASSCF levels disappears if dynamic electron correlation is included in the electronic structure model.

From Figure 1 it is not straightforward to deduce excited-state ν_{12} vibration frequencies and transition moments for absorption from the ground state. This is due to the limited extent of the data and the neglect of possibly significant harmonic and anharmonic couplings to other modes. The key experimental data concerning this mode is that *no* lines have been identified with it in one-photon absorption, but it has been observed at 636 cm^{-1} in two-photon absorption.[10,34,49] Kleier *et al.*[10] suggested that their valence-bond results may be consistent with these observations, the depth of the double-well being of the order of the zero-point energy of the oscillator. We test this suggestion quantitatively by extrapolating their data and performing a variational analysis. This calculation predicts that the zero-point level lies just below the barrier, with a one-photon forbidden level lying above it by +300 cm^{-1}. There exists an allowed one-photon transition to $2\nu_{12}$, however, and this is calculated at 1100 cm^{-1} with an intensity equal to 21% of the band-origin intensity. This could only be the case if there exists an error in the spectral assignment.[8] For potential surfaces of this general type, the qualitative feature of a $2\nu_{12}$ band with significant intensity appears robust; indeed, from the CASSCF results, lower vibration frequencies and larger overtone intensities are expected. The same variational approach applied to our (extrapolated) MRCI data predicts an excited-state ν_{12} vibration frequency of 550 cm^{-1}, close to the experimental frequency of 636 cm^{-1}. In one-photon absorption, a weak band corresponding to $2\nu_{12}$ at 1440 cm^{-1} is predicted, with an intensity of only 2.5% of the origin band. This is in a congested area of the spectrum[8] and would be difficult to identify. While these analyses are clearly quite approximate, they strongly suggest that the available experimental evidence indicates a delocalized single-well structure.

Another relevant question concerning the equilibrium geometry of S_1 is the possibility suggested experimentally[7] that a slight out-of-plane distortion occurs which lowers the symmetry to C_{2h}. Any such distortion must indeed be quite small as it is not obvious from the available inertial data.[80] Evidence for such a distortion is based on the appearance of apparent Franck–Condon progressions in an out-of-plane mode, but these progressions are quite short and alternative interpretations of the spectra are possible; our DZP-CASSCF calculations do not predict an out-of-plane distortion. As our calculated solvent shifts are insensitive to distortions of this type, we have not pursued this matter further.

(e) Gas-Phase Charge Distributions. In order to generate intermolecular potential functions, atomic charges are fitted[1] to reproduce the *ab initio* calculated molecular ESP over the region of the first few solvent coordination shells, specifically at all locations between 1.4 and 2.5 times the molecular van der Waals shell; for hydrogen-bonding problems, we use slightly modified[1] radii of 1.3, 1.7, and 1.2 Å for N, C, and H, respectively. In all, a total of eight different pyrazine–water potential functions are generated, all with the same Lennard-Jones interactions but with differing electrostatic terms. For the ground state these potentials are as follows: (1) Φ_{SCF}—fitted to S_0 SCF ESP using atomic point charges only; (2) $\Phi_{SCF/X}$—fitted to S_0 SCF ESP using atomic point charges as well as a point dipole on the nitrogen atoms and an additional set of floating point charges and dipoles X; (3) Φ_{CI}—fitted to S_0 CI ESP using atomic point charges only; and (4) $\Phi_{CI/X}$—fitted to S_0 CI ESP using atomic point charges as well as a point dipole on the nitrogen atoms and an additional set of floating point charges and dipoles X. For the excited state, analogous potentials called Φ'_{SCF}, $\Phi'_{SCF/X}$, Φ'_{CI}, and $\Phi'_{CI/X}$ are also generated, respectively,

(78) Dupuis, M.; Rys, J.; King, H. F. *J. Chem. Phys.* **1976**, *65*, 111.
(79) Werner, H.-J.; Knowles, P. J. MOLPRO program package.
(80) Innes, K. K.; Kalantar, A. H.; Khan, A. Y.; Durnick, T. J. *J. Mol. Spectrosc.* **1972**, *43*, 477.

Table 2. Atomic N, C, and H Charges Plus Additional Point Charges X, in e, as well as N and X Point Dipoles, in Debye, Used in the Various Pyrazine-Water Intermolecular Pair Potentials As Obtained by Fitting the *ab Initio* Calculated ESP

potentials	q_N	q_C	q_H	q_X	$\mu_{N,L}$	$\mu_{X,L}$	$\mu_{X,S}$	$\mu_{X,N}$
Φ_{SCF}	−0.4508	0.1260	0.0994	0	0	0	0	0
$\Phi_{SCF/X}$	1.7770	−0.0927	0.1767	−0.4863	∓5.5462	∓0.3202	±0.1590	±0.8581
Φ_{CI}	−0.4359	0.1382	0.0797	0	0	0	0	0
$\Phi_{CI/X}$	−0.4359	0.1381	0.0796	0.0001	∓1.3174	±0.3019	∓0.2573	∓1.6381
Φ'_{SCF}	0.3651	−0.6327	0.3063	0	0	0	0	0
	−0.5547	0.3476	0.0736	0	0	0	0	0
$\Phi'_{SCF/X}$	0.0208	−0.1561	0.2426	−0.8553	0.5046	2.0699	±0.5302	∓1.3735
	0.3377	−0.5150	0.2489	0.8555	2.6334	2.2207	∓0.8752	∓1.4787
Φ'_{CI}	−0.1683	−0.0712	0.1554	0	0	0	0	0
$\Phi'_{CI/X}$	1.8997	−0.2737	0.1741	-0.4251	∓4.9982	∓0.1368	∓0.1196	±0.7193

Table 3. Net Pyrazine Molecular Dipole Moments, in Debye, Traceless Quadrupole Moments, in Buckinghams, and the Root-Mean-Square Error, in kcal mol^{-1} e^{-1}, Resultant from the ESP Fitting Procedure for Each Intermolecular Potential as well as Values SCF-WF and CI-WF of the Moments Obtained Directly from the Electronic Wave Functions for Comparison

potentials	μ_L	B_{LL}	B_{SS}	B_{NN}	error
Φ_{SCF}	0	−10.9	14.1	−3.2	1.43
$\Phi_{SCF/X}$	0	−10.6	13.7	−3.1	0.22
SCF-WF	0	−10.7	13.8	−3.1	
Φ_{CI}	0	−10.4	12.8	−2.4	1.56
$\Phi_{CI/X}$	0	−10.0	12.3	−2.3	0.38
CI-WF	0	−10.2	12.4	−2.2	
Φ'_{SCF}	2.82	−5.4	12.4	−7.0	1.34
$\Phi'_{SCF/X}$	3.05	−5.0	12.0	−7.0	0.43
SCF-WF	2.87	−4.7	11.9	−7.2	
Φ'_{CI}	0	−5.2	11.1	−5.9	1.16
$\Phi'_{CI/X}$	0	−4.8	10.6	−5.8	0.37
CI-WF	0	−4.8	10.7	−5.9	

with the SCF potentials describing localized (n,π^*) excitations while the CI potentials reflect delocalization. The locations of the additional points X are also given in Table 1, while the fitted charges and moments are shown in Table 2 and the root-mean-square errors between the *ab initio* and fitted ESPs are shown in Table 3. Contours of the *ab initio* CI ESP for S_0 and S_1 sectioned both in the molecular plane and normal to it are shown in Figure 3, along with contours obtained from the charge distributions fitted to these data. In all cases, the fitted and *ab initio* ESPs at locations distant from the molecule are in excellent agreement; this is reflected in the comparison of the fitted and *ab initio* molecular dipole and quadrupole moments, and these are also shown in Table 3. Close to the molecule, higher moments are important, especially in the region of the first solvent coordination shell in solution. Because of the high symmetry of the D_{2h} structures, atomic-charge-only functions are not sufficiently flexible to reproduce the details of the ESP in important close-lying regions such as the hydrogen-bonding region. For this reason, the potentials containing the nitrogen point dipole and the additional point charge/dipole X are generated. However, the Lennard-Jones terms used in the intermolecular potentials are optimized for charge-only electrostatic interactions: adding additional terms, while improving the fit to the ESP, usually produces hydrogen-bonding intermolecular potentials which are far too attractive.[1]

It is not always possible to assign physical meaning to the values of the charges and dipoles shown in Table 2, the bottom line being that these distributions only serve to reproduce the ESP outside of the molecule. A useful comparison is of the nitrogen charge used in Φ_{CI} and Φ'_{CI}, being −0.43 e and −0.17 e, respectively. This shows that significant excess electron density remains on the nitrogen atoms in the excited state, a consequence of the tendency of the π^* orbital itself to lie on the nitrogen atoms rather than the carbon atoms.[43] For $\Phi'_{CI/X}$, the atomic charges themselves appear to be physically unreasonable, with e.g. the nitrogen charge being +1.9 e; this result is reasonable, however, when one considers that the 8 additional charges form two planes located 0.96 Å above and below the molecule and are used to explicitly represent and structure the π cloud.

(f) Molecular Polarizabilities. The solvent-shift calculations treat the solute as being polarizable, and require as input the molecular polarizability of pyrazine in both its S_0 and S_1 states. Ideally, these quantities should be evaluated using the above CASSCF/MRCI procedure. For this system, we find that the calculated solvent shifts are insensitive to the solute polarizability, and for reasons of computational efficiency we calculate it using finite field CNDO/S-CI calculations.[81] The results are (α_{LL}, α_{SS}, α_{NN}) = (53, 62, 13) au for S_0, the in-plane components being quite close to both the *ab initio* SCF results[82] of (68, 72, 39) au and the observed results[83] (assuming α_{LL}= α_{SS}) of (65, 65, 39) au; for S_1 the calculated polarizability is (125, 56, 13) au for a delocalized excitation and (98, 59, 12) au for a localized one.

3. Pyrazine−Water Clusters

Results obtained for the S_0 and S_1 states of pyrazine·H_2O and for the $S_0 \rightarrow S_1$ transitions in pyrazine·H_2O and pyrazine·$(H_2O)_2$ are shown in Table 4 using the four analogous pairs of potential surfaces. In all cases, stable ground-state linear N−H−O hydrogen bonds form; the bond energies obtained using $\Phi_{SCF/X}$ and $\Phi_{CI/X}$ are, as expected, ca. 3 kcal/mol deeper than those obtained using Φ_{SCf} and Φ_{CI}, respectively, due to the improved representation of the electrostatic interaction close to the nitrogen atoms that is apparent in Figure 3. The actual pyrazine−water dimer hydrogen bond energy is unknown but probably lies near 5 kcal/mol, approximately that predicted by $\Phi_{SCF/X}$ and $\Phi_{CI/X}$; typically,[1,74] condensed-phase effective pair potentials such as these overestimate the binding energy of gas-phase clusters by 1−2 kcal/mol. Low-lying isomers with the water molecule above pyrazine's molecular plane forming a type of hydrogen bond to the aromatic π cloud are found for Φ_{SCF} and Φ_{CI}, and the presence of associated low-lying transition states makes the linear hydrogen bonds flexible and facilitates easy isomerization.

In the excited state, Φ'_{SCF} and $\Phi'_{SCF/X}$ are electron localized and hence predict one very strong linear hydrogen bond per pyrazine, the hydrogen bond forming to the unexcited nitrogen atom. Alternatively, Φ'_{CI} and $\Phi'_{CI/X}$ delocalize the (n,π^*) excitation and support two equivalent but significantly weakened hydrogen bonds per pyrazine.

The only experimental data currently available for these clusters concerns the $S_0 \rightarrow S_1$ absorption spectra in neon matrix,[52] alcohol glass,[51] and a molecular beam.[53] In the neon matrix and the glass, vibrationally resolved high-resolution spectra are observed, indicating that both the mono- and dihydrates are stable in S_1, no new progressions are observed indicating that the N−H bond lengths change by less than 0.07 Å, and no spectral congestion occurs indicating that the excited-state dynamics produced by the Franck-Condon excitation is a regular, periodic motion. Qualitatively, only the results shown in Table 4 for the Φ_{CI} and $\Phi_{CI/X}$ pair are consistent with these

(81) Ellis, R. L.; Kuehnlenz, G.; Jaffé, H. H. *Theoret. Chim. Acta* **1972**, *26*, 131.
(82) Mulder, F.; Van Dijk, G.; Huiszoon, C. *Mol. Phys.* **1979**, *38*, 577.
(83) Battaglia, M. R.; Ritchie, G. L. D. *J. Chem. Soc., Perkin Trans. 2* **1977**, 897.

Table 4. Properties of Pyrazine·(H_2O) and Pyrazine·(H_2O_2) with all Energies in kcal/mol, Bond Lengths in Å, and Frequencies in cm^{-1} [a]

potentials for S_0, S_1		SCF	SCF/X	CI	CI/X	obs
S_1 localized?		yes	yes	no	no	
S_0 pyrazine·(H_2O)	HB symmetry	C_1	C_s	C_1	C_s	
	HB energy	−5.0	−8.1	−4.7	−7.3	
	πB energy	−4.1	none	−3.7	none	
	TS energy	−4.1	none	−3.7	none	
S_1 pyrazine.(H_2O)	HB symmetry	C_1	C_s		C_s	
	HB energy	−6.6	−8.2	none	−4.3	
	πB energy	none	−4.9	−4.6	−3.0	
	TS energy	none	−3.5	?	−3.4	
$S_0 \rightarrow S_1$ pyrazine·(H_2O)	$\lvert\Delta r_{NO}\rvert$	0.060	0.067	∞	0.094	<0.07[b]
	$\Delta\nu_{00}$	−530	−50	XX	1000	~470[c]
	$\Delta\nu_A$	−500	−20	900	1200	
	FC dynamics	periodic	periodic	chaotic	periodic	periodic[d]
$S_0 \rightarrow S_1$ pyrazine.(H_2O)$_2$	$\lvert\Delta r_{NO}\rvert$	∞	∞	∞	0.094	<0.07[b]
	$\Delta\nu_{00}$	XX	XX	XX	2000	1100[b]
	$\Delta\nu_A$	2600	3400	1800	2400	
	FC dynamics	dissoc	dissoc	chaotic	periodic	periodic[d]

[a] HB: linear hydrogen-bonded structure (the C_1 structures have the pyrazine and water planes pseudoparallel, the C_s structures have them precisely perpendicular). πB: structures with the water essentially hydrogen bonded to the aromatic π ring. TS: transition-state structures linking the HB and πB structures. none: no structure of this type was found. Δr_{NO}: change in the equilibrium NO bond length between HB structures. $\Delta\nu_{00}$: change in absorption origin frequency (XX indicates that the absorption band cannot be resolved into vibrational lines). $\Delta\nu_A$: change in the absorption band center evaluated using the effective pair potentials. FC dynamics: indicates the motion of the Franck−Condon excited ground-state wavepacket on the excited state surface, which may be either simple periodic motion, chaotic motion trapped for at least 20 ps in the excited state HB well, or dissociative, breaking the cluster in two. [b] Observed data taken from ref 52. [c] 350 cm^{-1} in solid neon[52] and 580 cm^{-1} in a molecular beam.[53] [d] Based[87] on the observation[52] of a regular high-resolution absorption spectrum.

Table 5. Properties of Dilute Pyrazine Solution[a]

potential	SCF	SCF/X	CI/X	obs
Is it localized?	yes	yes	no	
S_0 ΔH	−13.5[e]	−18.5[e]	−16.2[g]	−11.8[b]
S_0 ΔV	64[f]	58[f]	69[h]	70.8[c]
S_0 #HB	2.0	2.1	2.0	
S_1 ΔH	−9.4[e]	−14.4[e]	−7.9[g]	−10.7[b]
S_1 ΔV	76[f]	70[f]	78[h]	
S_1 #HB	1.5	1.0	0.5	
$\Delta\nu_A$	1900[e]	1800[e]	2000[g]	1600−2000[d]
ΔHWHM$_A$	600	1600	600	~500[d]
$\Delta\nu_F$	1800	2600	−300	−400[d]
ΔHWHM$_F$	900	1400	700	500[d]

[a] ΔH is the enthalpy of hydration, in kcal/mol; ΔV is the partial specific volume, in cm^3/mol, #HB is the average number of hydrogen bonds (i.e., N−H separations <2.5 Å) per pyrazine molecule, and $\Delta\nu_A$, $\Delta\nu_F$ are the changes, in cm^{-1} (estimated error ±100 cm^{-1}), in the electronic absorption and fluorescence band maxima, respectively, while ΔHWHM are the corresponding changes in the band half widths at half maximum. [b] From ref 84. [c] From refs 88. [d] From refs 13 and 36. [e] ±2 kcal/mol or 700 cm^{-1}. [f] ±10 cm^3/mol. [g] ±1.5 kcal/mol or 500 cm^{-1}. [h] ±6 cm^3/mol.

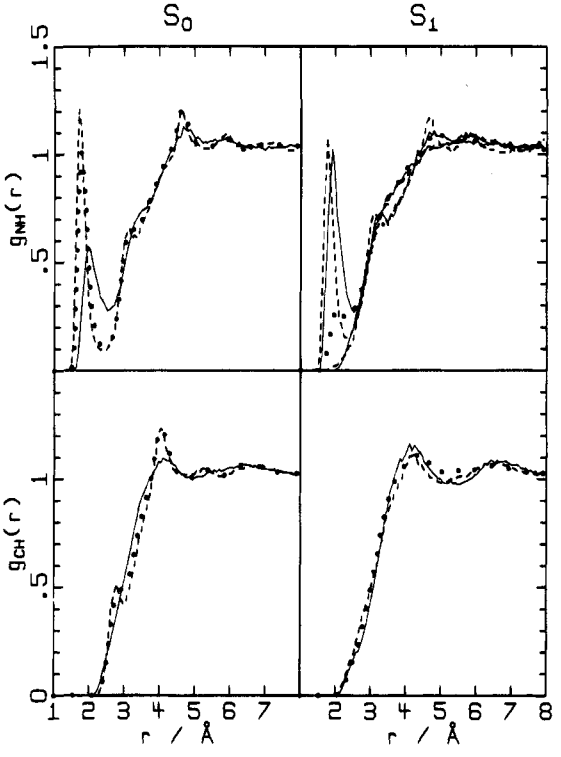

Figure 4. The calculated radial distribution functions $g(r)$ for pyrazine N or C to liquid-water H interactions obtained for pyrazine in its S_0 or S_1 electronic states: (−) from Φ_{SCF} and Φ'_{SCF} potentials; (- - -) from $\Phi_{SCF/X}$ and $\Phi'_{SCF/X}$ potentials; (●) from $\Phi_{CI/X}$ and $\Phi'_{CI/X}$ potentials.

experimental results, with the localized potentials predicting that the dihydrate is dissociative in its excited state. Quantitatively, this pair reproduces the small displacement in the N−H bond length very well, but overestimates the blue shift of the absorption band origin considerably and incorrectly treats the dihydrate formation as occurring in two essentially independent steps.

4. Results for Pyrazine−Water Solution

Results obtained for the structure, spectroscopy, and thermodynamics of water around pyrazine in its S_0 and S_1 electronic states are shown in Table 5, and pyrazine nitrogen or carbon to water hydrogen radial distribution functions $g(r)$ are shown in Figure 4. All potentials produce on average two hydrogen bonds per pyrazine in its ground state, consistent with qualitative experimental estimates.[84] This result is quite different from that obtained for dilute pyrazine solution obtained by Broo[85] by simulation using a molecular mechanics intermolecular potential: this calculation predicted that no pyrazine−water hydrogen bonds form at all, a result presumably attributable to a poor description of pyrazine's ESP within the potential surface. The most significant difference between our three simulation results is that Φ_{SCF} produces, presumably correctly, a longer and more flexible hydrogen bond than does $\Phi_{SCF/X}$ and $\Phi_{CI/X}$. Also, some

(84) Spencer, N. N.; Holmboe, E. S.; Kirshenbaum, M. R.; Barton, S. W.; Smith, K. A.; Wolbach, W. S.; Powell, J. F.; Chorazy, C. *Can. J. Chem.* **1982**, *60*, 1184.
(85) Boxer, S. G. *Photosynth. Res.* **1992**, *33*, 113.

structure is predicted by $\Phi_{SCF/X}$ in $g_{CH}(r)$. This is an artefact and arises from attractions between the additional points X which, in some sense, represent the π cloud and the water hydrogens; using an increased number of additional point charges is likely to reduce this effect, but the results serve to highlight problems which may arise when multi-parameter descriptions of the ESP are used.

Quantitatively, for S_0 the calculated enthalpies of hydration are overestimated somewhat compared to experiment. Naively, Φ_{SCF} would be expected to give the best result as the Lennard-Jones parameters used are optimized for this type of charge distribution, and it is found to overestimate the magnitude of the hydration enthalpy by 1.7 ± 2 kcal/mol; we have found that analogously derived potentials also overestimate the hydration enthalpy by 2.6 ± 2 and 1.7 ± 2 kcal/mol for pyrimidine[1] and pyridine[6] solutions, respectively. Representing the electrostatic interactions more precisely, as is done with the $\Phi_{SCF/X}$ potential, results in a considerable overestimate, as has also been found for pyrimidine[1] solutions, but the inclusion of electron correlation effects in $\Phi_{CI/X}$ does improve the results somewhat. Note that the error limits quoted in Table 5 reflect $1 - \sigma$ statistical uncertainties only and do not allow for possible small[1] systematic errors such as sample-size effects.

For the equilibrated excited state, the localized potentials Φ'_{SCF} and $\Phi'_{SCF/X}$ predict strong hydrogen bonding at one end and none at the other: Φ'_{SCF} even allows on average 1.5 water molecules to bond to the same pyrazine nitrogen atom. Alternatively, the delocalized potential $\Phi'_{CI/X}$ predicts that some weak residual hydrogen bonding remains at both nitrogens, with on average only 0.5 hydrogen bonds per pyrazine. The weakness of the excited-state hydrogen bonding is not attributed solely to the reduced bond energy, but also to the presence of energetically accessible regions in which the water molecules are competitively attracted to the excessively electron-rich π system. These alternative configurations, with a small spread in energies but with very different geometries, result in a poorly convergent Monte Carlo calculation; this affects not only the total energy (used here in the calculation of ΔH) but also the solvent−solute energy (used, e.g., in free-energy perturbation calculations).

Evaluated using our complete solvent-shift method, all potential pairs predict a solvatochromic shift of the center of the $S_0 \rightarrow S_1$ absorption band of around 1800 cm^{-1}, in good agreement with the observed value; only the SCF and CI/X pairs predict an increase in the absorption half-width at half-maximum (HWHM) in agreement with experiment, however. The most significant test of the appropriateness of the various potential surfaces is found to be the corresponding $S_0 \leftarrow S_1$ fluorescence band shift: use of either of the localized excited-state potentials Φ'_{SCf} and $\Phi'_{SCF/X}$ results in the calculation of a large blue fluorescence shift with sizable changes in bandwidth, in stark contrast to the observed small red shift and small bandwidth change. The observed properties are reproduced only when the delocalized excited state potential is used.

Historically,[13] it has been believed that the fluorescence solvent shift associated with localized pyrazine S_1 should actually be small and negative: as no hydrogen bond could be present on the nitrogen on which the excitation is localized, a situation analogous to that of pyridine was expected. This analogy is quite poor, however, with the fundamental difference arising from the change in the molecular *dipole* moment in each case: for pyridine, the S_0 dipole moment is[86] 2.2 D and the S_1 moment is[45] 0.5 D, while for pyrazine these values reverse, being, from Table 3, 0 and 2.9 D, respectively. Hence, from the perspective of dielectric solvation, pyrazine *fluorescence* is analogous to pyridine *absorption*. Dielectric solvation and specific interaction terms contribute[3,6,13] equally to the solvent shift for pyridine and pyrimidine, and our results for pyrazine reflect contributions of similar magnitude. The important difference is that for pyridine the two contributions are large and add in absorption while both are small in emission; for localized pyrazine the reversed dipolar properties result in only specific bonding contributing to absorption with dielectric solvation contributing instead to the fluorescence solvent shift, rendering it moderately large and positive.

5. Conclusions

A consistent analysis is presented of the electronic structure of the S_1 state of pyrazine in the gas phase, in small water clusters, and in dilute aqueous solution. In all cases, one sees clear evidence that the localized (n,π^*) excitations interact strongly, producing a fully delocalized excited state with no $D_{2h} \rightarrow C_{2v}$ distortion. In the gas phase, while valence-bond and CASSCF calculations favor distortion, Davidson-corrected CASSCF-MRCI calculations strongly suggest that indeed no distortion occurs; further, vibrational analyses indicate that only a high-symmetry structure is consistent with the available high-resolution spectroscopic data. In small molecular clusters, high-resolution spectroscopy shows that doubly hydrogen-bonded clusters are stable in the excited state, and we show that this is only possible if the (n,π^*) excitation remains delocalized; the excited-state hydrogen bonds are seen to be only slightly weaker than those of the ground-state bond and have very similar equilibrium geometries. Further, in the liquid state, we find that *only* a high-symmetry delocalized description of S_1 can account for the observed fluorescence solvent shift, and that in *this* phase, very little hydrogen bonding occurs to S_1 not because the hydrogen bond is intrinsically absent but rather because non-hydrogen bonded structures involving interactions with the overly electron-rich π cloud have become competitive.

Acknowledgment. J.Z. and J.R.R. gratefully acknowledge support provided by the Australian Research Council for this project, and C. W. similarly acknowledges support from the Deutsche Forschungsgemeinschaft; the large *ab initio* calculations were performed on a Cray Y-MP8 at the Leibniz Rechenzentrum der Bayerischen Akademie der Wissenschaften. We thank Dr. J. S Craw (University of Manchester) and Dr. G. B. Bacskay (University of Sydney) for helpful discussions and advice concerning the use of quantum-chemical techniques.

Registry Numbers supplied by author: pyrazine, 290-37-9; pyrazine·H_2O, 66822-80-8; pyrazine·$(H_2O)_2$, 70937-99-4.

JA950819Q

(86) Sørensen, G. O.; Mahler, L.; Rastrup-Andersen, N. *J. Mol. Struct.* **1974**, *20*, 119.
(87) Heller, E. J.; Stechel, E. B.; Davis, M. J. *J. Chem. Phys.* **1980**, *73*, 4720.
(88) Enea, O.; Jolicoeur, C.; Hepler, L. G. *Can. J. Chem.* **1980**, *58*, 704.